Carbohydrate Research 344 (2009) 1235–1247

Contents lists available at ScienceDirect

Carbohydrate Research

journal homepage: www.elsevier.com/locate/carres

The (α-1,6) glycosidic bond of isomaltose: a tricky system for theoretical conformational studies

Fábio Javaroni, Aurélio B. B. Ferreira, Clarissa O. da Silva *

Departamento de Química, Universidade Federal Rural do Rio de Janeiro, Rodovia BR465, km 47, Seropédica, Rio de Janeiro, CEP 23.890-000, Brazil

ARTICLE INFO

Article history:
Received 17 February 2009
Received in revised form 19 April 2009
Accepted 21 April 2009
Available online 24 April 2009

Keywords:
Isomaltose conformers
Isomaltose potential energy surfaces
Alpha 1,6 glycosidic bond

ABSTRACT

Stable conformations of β-isomaltose (α-D-glucopyranosyl-(1→6)-β-D-glucose) in gas-phase and aqueous solution are investigated in this study using quantum mechanical calculations. Conformational maps are calculated at HF/6-31G(d,p) level and lower energy structures are sampled in the most stable regions. Entropic and thermal corrections are considered and the Boltzmann population is obtained for conformers that are representative of the 18 most stable regions found on the potential energy surface. B3LYP/6-31+G(d,p) and B3LYP/6-311+G(2d,2p) calculations are used in conformational samplings. Solvation effects are considered through the polarizable continuum model approach. Hydroxymethyl group orientations are investigated for the most stable conformers. The influence of electronic correlation and solvation on the glycosidic linkage preference (TG, GT, and GG) and hydroxymethyl group orientation (*tg*, *gt*, and *gg*) are discussed. Heteronuclear spin coupling constants ($^3J_{C,H}$) along the glycosidic linkage are calculated and comparison with other theoretical results and experiments is used to validate the obtained structures.

1. Introduction

In this study, the investigation of the most stable conformations of the disaccharide α-D-glucopyranosyl-(1→6)-β-D-glucose, hereinafter referred to as β-isomaltose, is performed through ab initio calculations. From a practical point of view, this disaccharide is generally used as a prototype of the starch and glycogen branching, once branching in these polymers occurs through an α-(1→6) bond between two glucose residues of the polymeric chain (Fig. 1).

Because conformational studies of carbohydrates are a keystone in the carbohydrate field,[1] there are many published papers devoted to similar purposes and other disaccharides. The large majority of them (just to cite those related to isomaltose) use classical[2–4] or semi-empirical[5] methods to obtain stable conformations. In fact, classical techniques are very powerful and particularly useful when the system is too large, very flexible, or the phenomenon studied does not involve stereo electronic effects. However, the latter is exactly the case: according to previous studies, in disaccharides the ϕ angle is defined by the exo-anomeric effect[6] and the ψ angle by non-bonded interactions.[7] An interesting comparison among the most used force fields dedicated to conformational studies of carbohydrates was performed by Engelsen and co-workers,[8] and Pérez et al.[9] The final conclusion is that we have not reached yet an acceptable level of parameterization of force fields able to describe either the exo-anomeric effects or the stabilization energy from an intermolecular hydrogen bond. Both effects are extremely important in determining conformation in carbohydrates and, therefore, from our point of view, preclude the use of non-specific force fields to investigate the conformational aspects of these systems in detail.

On the other hand, ab initio descriptions are very efficient in quantifying stereo electronic effects because no parameterizations are used to calculate electronic potentials. In fact, quantum mechanical descriptions can nowadays be extended to larger systems than those described 20 years ago due to two correlated facts: (a) we now have at our disposal very fast computers and, consequently, (b) very efficient computational codes were developed, which were able to deal with larger systems. Such a situation allows the adoption of a quantum approach to systems of a reasonable dimension (as a disaccharide), within an acceptable range of time.

In this context, the problem of accessing the quantum mechanical energy of a disaccharide is solved.[10,11] However, there remains the physical question related to its huge flexibility that is mathematically expressed as a potential energy surface with a high density of minima. By the adoption of ab initio models, we can determine very precisely the depth of each minimum but it is extremely important to assure that the most stable conformations are comprised in the potential energy surface. Clearly, it is an intrinsic characteristic of these systems and, therefore, a protocol must be established in order to avoid non-representative conformational sampling. In other words, it is important to look for any hierarchy with respect to the energy among the degrees of freedom of the disaccharides.

* Corresponding author. Tel./fax: +55 21 26822807.
E-mail address: clarissa-dq@ufrrj.br (C.O. da Silva).

0008-6215/$ - see front matter © 2009 Elsevier Ltd. All rights reserved.
doi:10.1016/j.carres.2009.04.022

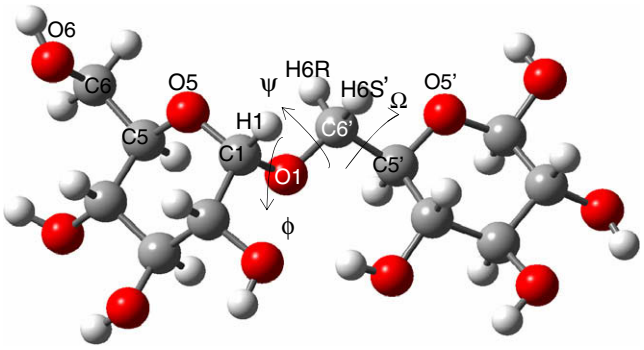

Figure 1. Definition of the dihedral angles ϕ (O5–C1–O1–C6′), ψ (C1–O1–C6′–C5′), and Ω (O1–C6′–C5′–O5′) in the β-isomaltose, a disaccharide with an α-(1→6) glycosidic linkage.

Moreover, a theoretical study on carbohydrates conformation can provide unique information because the available experimental data for carbohydrate in solution is always an average value. Therefore, it is impossible to recover the individual contributions from them because two sets of variables are ignored: each relevant conformation (at a certain temperature, pressure, and medium) and its individual contribution to the property.

First proposed by Lemieux and Koto,[12] and afterwards recognized by important studies,[13] the most relevant geometrical parameters to define the three-dimensional structure of disaccharides are the dihedral angles (ϕ and ψ) of the glycosidic linkage. French et al.[14] mention the necessity of a reliable technique for scanning such angles in a study dedicated to describe crystalline structures. In the case of the 1→6 bond, a third dihedral angle called Ω needs to be specified, in order to univocally define the relative monosaccharidic orientations (Fig. 1). Such degrees of freedom must be properly investigated by the adopted description; otherwise, as already mentioned, the final obtained structures will not be a representative ensemble of the β-isomaltose compound. Previous studies using ab initio calculations to obtain potential energy surfaces[15,16] to sample conformers on them and also to calculate kinetic[17] and optical properties[18] of carbohydrates encouraged us. This is because they furnished theoretical values for them which are in better agreement with the experimental data than those obtained when classical methods were employed in the sampling of stable structures. However, such studies were performed for monosaccharides or disaccharides with 1→1 and 1→4 glycosidic linkages, and the protocol adopted in these cases needs to be tested for the more flexible 1→6 bond.

Surprisingly, despite the importance of the isomaltose, few published studies can be found that really provide insights into its most abundant conformations. Among the most important contributions, we can detail two studies. In the first, Pérez and co-workers[5] have performed semi-empirical calculations for the isolated molecule in four different solvents. The results obtained identified 15 stable conformers on the potential energy surface of this carbohydrate and relative population in vacuum for the structures with orientation gauche–gauche (GG), gauche–trans (GT), and trans–gauche (TG) of 71%, 17%, and 12%, respectively, corresponding to values of 300°, 60°, and 180° for the dihedral Ω angle of the glycosidic bond. For the same parameters in an aqueous solution, the relative distribution found was 52%, 31%, and 12%. In the second study, Dowd et al.[3] used molecular mechanics (MM3) calculations to finally identify 13 structures (7 for alpha and 6 for beta anomers) with the GT orientation for the glycosidic bond preferred over the GG orientation in the set of obtained conformations.

A central question always present in conformational studies of carbohydrates in general regards the proper consideration of solvation effects. Our first choice is to describe the β-isomaltose (which has a higher dipole moment than the α-anomer and, therefore, could be more sensitive to solvation effects than the latter) in an aqueous solution through a polarizable continuum model. We recognize that sometimes this kind of approach may not be suitable to reproduce solvent effects and explicit solvent molecules must be added to the solute, principally when dynamical aspects play a central role.[19] Here it is not the case and by adopting this model we are tacitly assuming that we are describing the molecule in an aqueous solution, after the thermodynamic equilibrium is reached. It is the same to assume that the conformations considered resemble those of larger residence time in a molecular dynamic simulation. Such correspondence is possible because the electrostatic effects mostly govern the interaction of carbohydrates and water due to the high dielectric constant of water and to the high dipole moments of the hydroxymethyl groups present in a large number in the carbohydrate structure. Therefore, hydrogen bond interactions, although with well-defined orientations, can also be included among the electrostatic interactions because, as suggested,[20] its largest component is of an electrostatic nature.

In fact, solvation is a delicate task for carbohydrates in general, as highlighted by the renowned study of Kirschner and Woods.[21] In that study, the authors concluded that molecular mechanics simulations are better than quantum mechanical calculations to reproduce the experimental[22] relative abundance of GT, TG, and GG rotamers in the aqueous solution of methyl α-D-glucopyranoside and methyl α-D-galactopyranoside. Because the simulations are based on force-field parameters derived from gas-phase data,[23] interactions with explicitly included water must be responsible for the resultant gauche population preference. The primary role of water, according to the authors, appears to be to weaken the internal hydrogen bonds of the carbohydrates. Due to these important observations, it is mandatory to properly take into account solvation effects to describe isomaltose conformers. Additionally, once the vapor pressure of carbohydrates can be neglected at room temperature, the large majority of experimental results for carbohydrate properties are obtained in aqueous solution. Therefore, to validate the set of conformers obtained through the comparison of any property calculated from the selected set and its corresponding experimental value, a more realistic description of these systems has to consider the solution phase. Instead of comparing geometries of the most stable conformers obtained in this study with those already published,[3,5] we believe that a comparison with an experimental property is much more useful. Accordingly, the properties used to validate the conformational sampling proposed here are the heteronuclear spin coupling constants ($^3J_{C,H}$) across the glycosidic linkage.

2. Methodology

2.1. Calculations

Conformational maps were calculated for β-isomaltose in gas-phase at HF/6-31G(d,p) level.[24] The extensive studies of Lii et al.[25] on potential energy surfaces of more than 80 conformers (D-aldo and D-ketohexoses) show the importance of considering diffuse functions for heavy atoms into the basis set, if density functional theory is used. Csonka[24] also confirmed these findings and showed, however, that HF/6-31G(d) is already an acceptable description, once intramolecular hydrogen bonds energies are well described at this level of calculation. These studies were performed on monosaccharides but it is our goal to establish the simplest possible ab initio protocol to generate reliable conformational maps for disaccharides. As for disaccharides, the location of the stability regions in conformational maps was proved to be the same in both descriptions[15] and conformational maps were calculated at the HF/

6-31G(d,p) level. In order to evaluate how sensible conformations are to the level of theory used, B3LYP/6-31+G(d,p) and B3LYP/6-311+G(2d,2p) calculations were used in sampling in the stability regions of the aforementioned maps.

To introduce solvent effects, we have used the polarizable continuum model[26] (PCM) in its integral equation formalism (IEFPCM) formulation.[27] In this approach, the solvent is described as a dielectric continuum medium, polarized by the presence of the solute. In this model the solute molecule is placed inside a cavity opened in the dielectric. Its shape takes into account the geometry of the molecule. The polarization charges that imitate the solvent polarization due to the presence of the solute are located on the surface of the cavity on small area units called *tesserae*. In the present case, the molecular cavity was built from interlocking spheres centered on selected atoms or groups of atoms. The radii of the spheres are as follows: 2.28 Å for a CH or CH_2 group, 1.80 Å for an O atom, and 1.44 Å for an H bonded to oxygen atom of the hydroxyl groups.[28] The solvation energy of the system was computed and expressed as a summation of four components: electrostatic, dispersion, repulsion, and cavitation. The calculations with PCM follow two descriptions: single point calculations on the geometries found in the gas-phase, which is an inclusion of the solvent effects only on the energy, and geometry optimizations considering the solvent effects. The comparison of such procedures is useful to distinguish between the role of solvent effects on the geometry and on the relative energies of the system (and consequently on the Boltzmann population), separately.

Calculations of vibrational frequencies were carried out for the final structures in the gas-phase and in solution to properly characterize them as stationary points of minimum energy and to make possible the introduction of thermal and entropic corrections.

All the calculations used to build the conformational maps were performed in the JAGUAR program.[29] The conformational maps were obtained from the interpolation of the respective energy data using the Radial Basis Function method. The GAUSSIAN 03[30] code was used in the geometry optimization calculations related to sampling in the stability regions of the maps and to consider the solvent effects.

Finally, the validity of the structures obtained was tested by computing the heteronuclear spin coupling constants ($^3J_{C,H}$) across the glycosidic linkage, a property very sensitive to small variations of the angles ϕ, ψ, and Ω. By comparison with experimental data, it is possible to evaluate how well the ensemble of the obtained conformers describes the β-isomaltose compound. The heteronuclear spin coupling constants ($^3J_{C,H}$) were calculated through the Karplus-type equations[31,32] reported below, where H6R′ and H6S′ refer to prochiral hydrogen atoms (see Fig. 1):

$$^3J_{C6',H1} = 5.7\ \cos^2(\phi_{H1}) - 0.6\ \cos(\phi_{H1}) + 0.5,$$
where $\phi_{H1} = (H1{-}C1{-}O1{-}C6')$

$$^3J_{C1,H6R'} = 5.7\ \cos^2(\phi_{H6R'}) - 0.6\ \cos(\phi_{H6R'}) + 0.5,$$
where $\phi_{H6R'} = (H6R'{-}C6'{-}O1{-}C1)$

$$^3J_{C1,H6S'} = 5.7\ \cos^2(\phi_{H6S'}) - 0.6\ \cos(\phi_{H6S'}) + 0.5,$$
where $\phi_{H6S'} = (H6S'{-}C6'{-}O1{-}C1)$.

$$^3J_{C4',H6R'} = 5.8\ \cos^2(\phi_{H6R'}) - 1.6\ \cos(\phi_{H6R'}) + 0.28\ \sin(2\phi_{H6R'}) - 0.02\ \sin(\phi_{H6R'}) + 0.52,$$
where $\phi_{H6R'} = (H6R'{-}C6'{-}C5'{-}C4')$

$$^3J_{C4',H6S'} = 5.8\ \cos^2(\phi_{H6S'}) - 1.6\ \cos(\phi_{H6S'}) + 0.28\ \sin(2\phi_{H6S'}) - 0.02\ \sin(\phi_{H6S'}) + 0.52,$$
where $\phi_{H6S'} = (H6S'{-}C6'{-}C5'{-}C4')$

The same set of coupling constants was also calculated from ab initio methods,[33–35] as implemented in GAUSSIAN 03.[30]

2.2. Starting structure and map calculation

In order to explain the protocol adopted to obtain the potential energy surfaces for β-isomaltose, it is important to distinguish the ϕ and ψ angles from the Ω angle in a 1→6 glycosidic bond. While a change in the values of the formers implies a rotation of a C–O bond, the same change in the latter implies a rotation of a C–C bond. In the first case, it is difficult to say which conformations are the most stable due to the electronic lone pairs of the O atom. For a C–C bond type, however, the sp^3 carbon hybridization imposes basically three possible values for this Ω angle: 60°, 180°, and 300°, in conformations called respectively GT, TG, and GG (due to steric effects, small deviations from these values can be accepted). As a priori, there is no reason to preclude any of these orientations, three different conformational maps were calculated for β-isomaltose. Each describes how the energy of the system changes with ϕ and ψ angles for a given Ω angle. This later was not frozen but checked for each structure obtained after the geometry optimization step. It was kept at the same value during the entire calculation. From now on, each map will be referred to as TG, GT, and GG, depending on the Ω angle value for the O1–C6′–C5′–O5′ sequence of the structures used to build it.

The initial geometry of β-isomaltose used in this study was obtained as follows: The monosaccharides (α-D-glucose and β-D-glucose) were built and their energies were minimized by geometrical optimization using a Dreiding II force field.[36] The two structures were connected through an α-(1→6) linkage in a GT orientation regarding the Ω angle, creating the desired disaccharide. The geometry of such structure was fully optimized in a molecular mechanics calculation using again Dreiding II and the resulting geometry was used as the starting geometry (Fig. 2) to build the corresponding GT conformational map. The same procedure was repeated twice, to obtain the TG and GG (regarding the Ω angle) starting structures reported in Figure 2, and used to build the respective TG and GG maps as explained in the next paragraphs.

Another important degree of freedom of β-isomaltose is the rotation of the hydroxymethyl group. The orientations *gt*, *tg,* and *gg* of the C5–C6 bond rotation are quantified by the dihedral angle (ω) defined for the O6–C6–C5–O5 sequence of atoms, as 60°, 180°, and 300°. The lowercase classification *gt*, *tg,* and *gg* is adopted for the hydroxymethyl orientations (ω) while the uppercase classification GT, TG, and GG is used for the glycosidic linkage (Ω). In all the starting structures, as well as in all calculations used to build the conformational maps, the hydroxymethyl orientations are *gg*. The hydroxymethyl rotation is a degree of freedom assumed as having a hierarchal position lower than the glycosidic angles rotation in the stabilization of the system.

This assumption is supported by the fact that the height of the barrier for hydroxymethyl group rotation is lower than the corresponding barriers for the glycosidic linkage rotations. The investigation of the hydroxyl orientations is not performed in this study.

For each starting structure, systematic rotations on the C–O bond were introduced in a scanning procedure of ϕ and ψ angle values. This means that each ϕ and ψ angle, at this time, was changed in 12 successive steps with increments of 30°. During each calculation, the ϕ and ψ angles were kept fixed, while all the other geometrical parameters of the molecule were optimized to minimize the energy. Then, three different conformational maps for β-isomaltose were built by interpolating a set of data comprising 144 energy values for each GT, GG, and TG conformation, called relaxed maps. Conformational sampling was performed in these maps, in the regions of minimum energy.

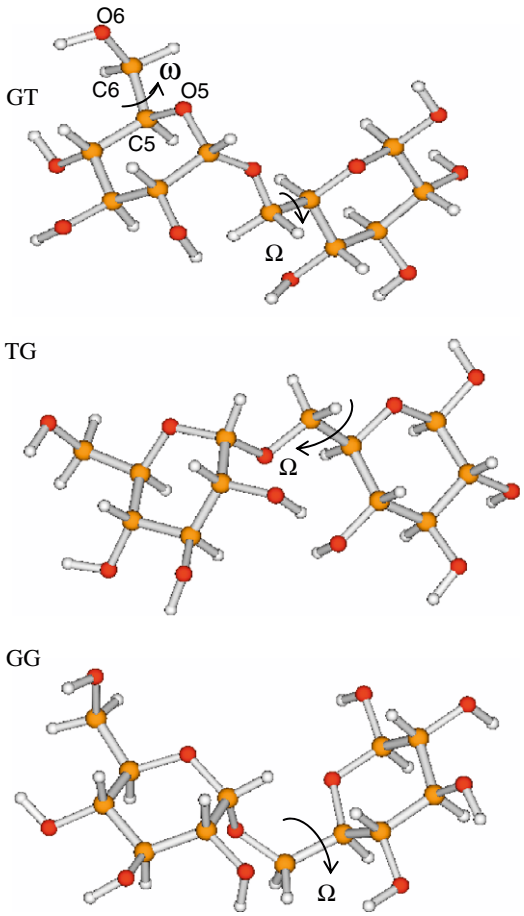

Figure 2. The starting geometries used in the calculations of the conformational maps. The values for the ϕ, ψ, and Ω angles in degrees are, respectively for GT = 230°, 155°, and 60°, for TG = 111°, 175°, and 180°, and for GG = 157°, 295°, and 300°.

Different conformations were built with dihedral angles initially settled by values of ϕ and ψ found in the regions of minimum energy, obtained from inspection in the conformational maps. Such structures had all geometrical parameters optimized, except the dihedral angles ϕ, ψ, and Ω, which were kept frozen during this calculation step. In a successive optimization step, such angles were also relaxed and the geometry of the structure fully optimized.

The final structures were solvated in single-point calculations and in geometry optimized calculations in the continuum to imitate the presence of the solvent, when properly mentioned.

The vibrational frequencies within the harmonic approximation were obtained for the final structures in the gas-phase to properly characterize them as stationary points of minimum energy, as well as to introduce thermal and entropic corrections. The Boltzmann population was calculated and for those structures with relative abundance larger than 1%, the rotation of the hydroxymethyl group was investigated.

3. Results and discussion

3.1. Relaxed conformational maps in the gas-phase

A total of 36 regions of stability were found for the three maps calculated for β-isomaltose, 11 for TG, 13 for GT, and 12 for GG map. The conformational maps are shown in Figures 3–5.

The gray-shaded regions of the potential energy surface labeled with letters correspond to regions of minimum energy and are defined by the pair of values for ϕ and ψ of the conformations with low energy, whose values are reported in Table 1.

From the conformational maps exhibited in Figures 3–5, the (1→6) glycosidic bond shows a very large number of stable relative orientations of the monosaccharidic units, as supposed to be possible for a disaccharide where steric hindrance can be avoided by more geometrical arrangements than those possible for shorter glycosidic bonds. It is important to recall that although a given orientation defined by the values of ϕ and ψ can appear in a stable region on the potential energy surfaces of Figures 3, 4, or 5, its occurrence is determined by the relative depth of the region regarding the global minimum, as well as by the temperature, as further explained in the next sections.

3.2. Optimization of the 36 structures in the gas-phase, obtained from the relaxed ab initio conformational maps

In our assumptions, the center of each stability region obtained from the three maps described in Section 3.1 defines values of dihedral angles that correspond to the stable geometrical arrangements of the two rings in β-isomaltose disaccharide. Such conformations were built and their energies minimized, in two steps as previously described. During the final energy minimization step, many conformers were converted into others, decreasing from 36 to 18 the number of stable representative structures. For these 18 structures, the angles ϕ, ψ, and Ω are reported in Table 2.

Compared to other (1→4)[15] and (1→1)[16] glycosidic bonds of disaccharides, it can be said that the sequence C1–O1–C6′–C5′ of a (1→6) disaccharide is more conformationally versatile, independent of the level of description considered. In such conformations, from Table 2 it can be seen that the ϕ angle is in most conformations approximately 60° and 300° in all structures, due to the exo-anomeric effect manifestation, while the Ω angle is approximately 60°, 180°, and 300° (conformations GT, TG, and GG, respectively). The ψ angle has the largest variation among these three degrees of freedom.

In order to properly characterize the structures obtained, as well as to obtain their relative abundance as a Boltzmann population, thermal and entropic corrections were considered, and the obtained results reported in Table 3 for both levels of theory studied.

From Table 3, it can be seen that only four structures (TG-A, GT-C, GG-B, and GG-C) have relative abundance larger than 0.5%, in the gas-phase at 298 K. Such structures are reported in Figure 6 and although the vapor pressure of β-isomaltose can be neglected at room temperature, their consideration is important because only intramolecular effects are taken into account in the stabilization of such conformations, once they are described as isolated molecules.

As can be seen from Table 3, the relative abundance is 84% for TG (A), 15% for GG (B + C), and less than 1% for GT (C) orientation along the glycosidic linkage, for the isolated molecule at HF/6-31G(d,p)level.

Single point B3LYP/6311+G(2d,2p) calculations (see Supplementary data for details) were performed on the same set of 18 conformers in the gas-phase—the thermal and entropic corrections were kept the same obtained at the HF/6-31G(d,p) level, once they should refer to the optimized geometry. In a successive step, geometry optimizations and frequency calculations on these 18 structures were conducted at the B3LYP/6-31+(d,p) level, and finally on the B3LYP/6311+G(2d,2p) level on these later geometries. The final results for conformational abundance are reported in Table 4.

From Table 4, it can be seen that the consideration of electronic correlation effects only on the energy changes to the relative population TG:GG:GT from 84:15:1 to 54:39:6. An increase of the GG conformer when electronic correlation effects are introduced only

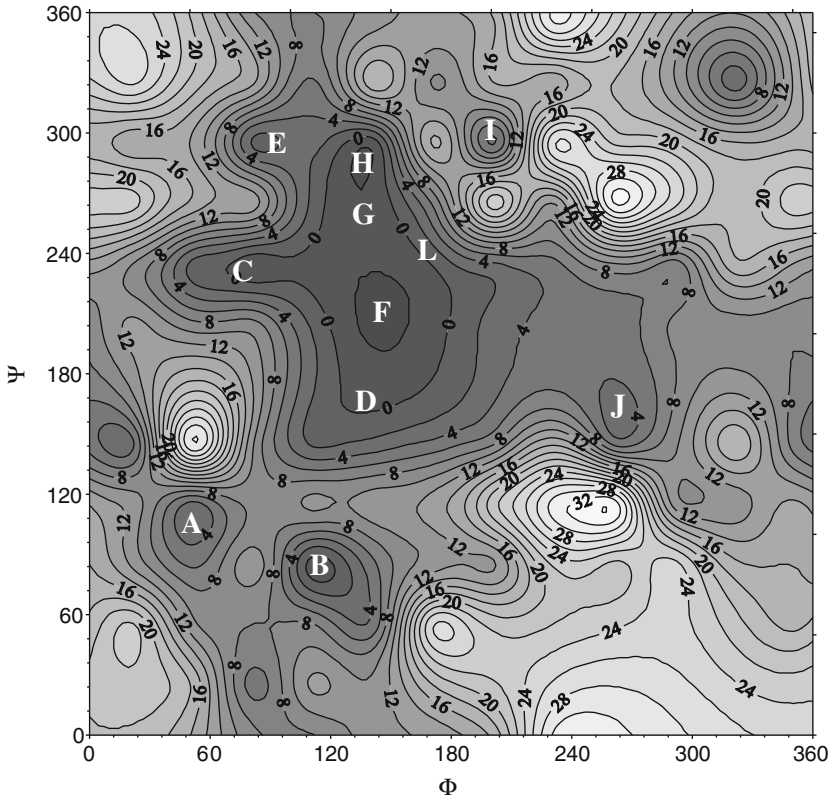

Figure 3. Relaxed conformational map calculated for TG β-isomaltose, by interpolation of a set of data obtained from 144 HF/6-31G(d,p) calculations. The energy values are in kcal/mol.

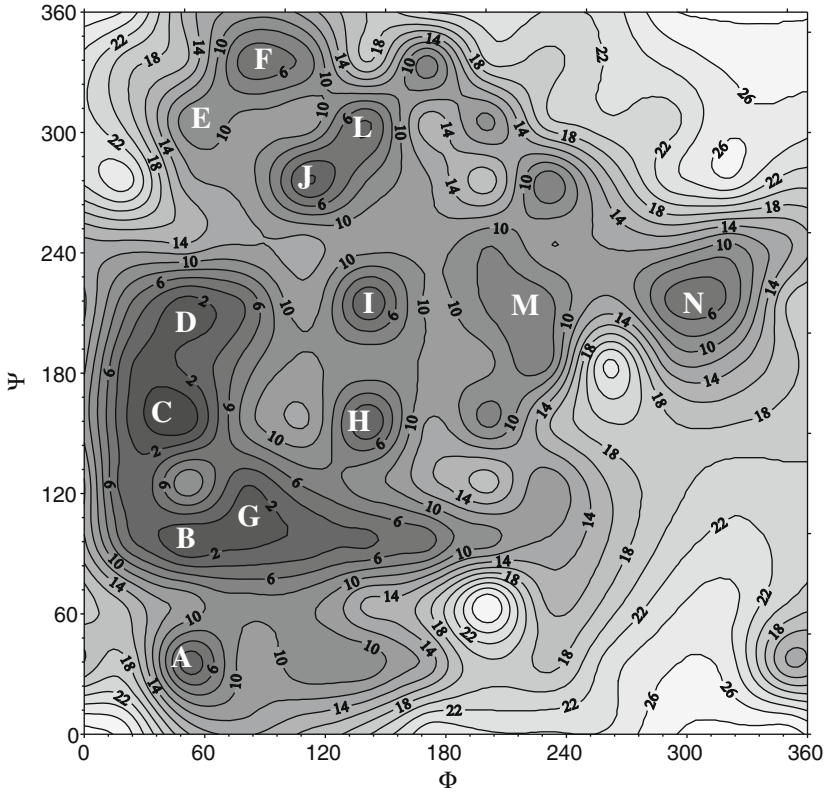

Figure 4. Relaxed conformational map calculated for GT β-isomaltose, by interpolation of a set of data obtained from 144 HF/6-31G(d,p) calculations. The energy values are in kcal/mol.

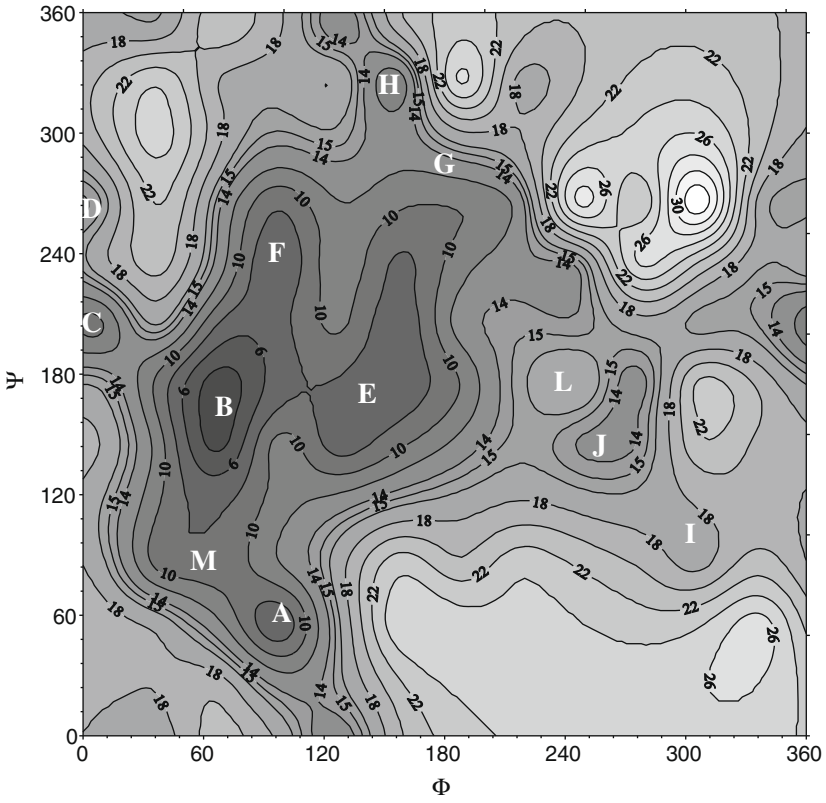

Figure 5. Relaxed conformational map calculated for GG β-isomaltose, by interpolation of a set of data obtained from 144 HF/6-31G(d,p) calculations. The energy values are in kcal/mol.

Table 1
Regions of stability found on the conformational maps described in Figures 3–5

Region	TG		GT		GG	
	ϕ (°)	ψ (°)	ϕ (°)	ψ (°)	ϕ (°)	ψ (°)
A	50	115	51	35	97	55
B	110	85	51	95	67	175
C	80	235	51	155	7	205
D	140	175	51	215	7	265
E	80	295	81	305	157	175
F	140	205	111	335	97	235
G	140	265	111	95	187	265
H	140	295	141	155	157	325
I	200	295	141	215	307	85
J	260	145	111	275	250	145
L	170	235	141	305	240	175
M	—	—	201	215	67	85
N	—	—	321	215	—	—

Table 2
Dihedral angles ϕ, ψ, and Ω obtained after full optimization of all geometrical parameters in the gas-phase, in degrees

Region	HF/6-31G(d,p)			B3LYP/6-31+G(d,p)		
	ϕ	ψ	Ω	ϕ	ψ	Ω
TG-A	77	159	181	82	154	180
TG-B	79	120	159	93	109	150
TG-C	76	246	181	76	244	183
TG-E	108	293	177	105	297	177
TG-J	258	187	182	267	185	182
TG-L	145	268	186	146	262	185
GT-B	92	74	47	97	75	48
GT-C	65	195	69	67	194	72
GT-E	94	293	75	92	295	79
GT-I	140	187	71	142	189	76
GT-L	113	279	69	107	285	77
GT-N	311	212	66	299	220	69
GG-A	75	85	275	78	83	273
GG-B	77	162	297	77	161	293
GG-C	69	179	295	72	178	295
GG-E	142	193	283	143	193	280
GG-F	96	244	288	94	247	286
GG-M	68	90	285	67	89	286

on the energy parallels an impressive decrease of the TG conformers' abundance. If electronic correlation effects are introduced also in the geometry, that is, if geometry optimizations and frequency calculations on these 18 structures are conducted at the B3LYP/6-31+(d,p) level, the final relative abundance is 61:35:4. If such effects are recovered on the energy using a larger basis set, the final result is 33:57:9. As density functional theory is a variational method, there is no doubt that the final result is superior to the HF/6-31G(d,p) method and it shows that TG conformers, still for the isolated molecule, became less stable than GG conformers. It is important to mention that no appreciable change was presented in the conformers of Figure 6, when the geometry is optimized at the B3LYP/6-31+(d,p) level, that justifies a new figure. Up to now, as no solvation effects were introduced, it is not possible to make comparisons with experiments.

However, such findings analyzed together with those found by Kirschner and Woods,[21] can bring more information about conformational aspects of 1,6 bond-like disaccharides: in that study the authors calculated potential energy curves for methyl α-D-glucopyranoside and methyl α-D-galactopyranoside, using molecular mechanics (AMBER/GLYCAM) and quantum mechanical (HF/6-31G(d) and B3LYP/6-31++(2d,2p)) calculations. Scanning the hydroxymethyl orientation in the 0–330° range, they allowed and disallowed (through a geometrical constraint) the intramolecular

Table 3
Glycosidic angles (in degrees), relative energies (in kcal/mol), Boltzmann population and dipole moment (in debye) for the 18 conformers obtained after full geometrical optimization of the structures sampled in the conformational maps of Figures 3–5, at HF/6-31G(d,p) and B3LYP 6-31+G(d,p) levels

Region	HF//6-31G(d,p)				B3LYP//6-31+G(d,p)			
	$\Delta U_{T=0\,K}$[a]	ΔG_{corr}[b]	ΔG_f^{gas}[c]	p^{gas} (%)	$\Delta U_{T=0\,K}$[d]	ΔG_{corr}[e]	ΔG_f^{gas}[c]	p^{gas} (%)
TG-A	0.00	0.00	0.00	83.81	0.00	0.00	0.00	60.19
TG-B	3.78	−0.13	3.65	0.18	3.02	0.05	3.07	0.34
TG-C	6.10	−0.40	5.70	0.01	5.57	−0.71	4.86	0.02
TG-E	6.57	0.62	7.19	0.00	5.51	0.43	5.94	0.00
TG-J	11.62	−0.50	11.12	0.00	9.50	−0.73	8.77	0.00
TG-L	5.31	−0.76	4.54	0.04	5.10	−1.02	4.09	0.06
GT-B	3.93	0.11	4.05	0.09	3.04	0.09	3.13	0.30
GT-C	3.35	−0.56	2.79	0.75	2.81	−1.16	1.65	3.71
GT-E	5.68	−0.33	5.35	0.01	4.84	−0.82	4.03	0.07
GT-I	8.06	−1.66	6.40	0.00	6.90	−1.87	5.04	0.01
GT-L	7.27	−0.99	6.80	0.00	6.77	−1.12	5.64	0.00
GT-N	12.87	−0.44	12.42	0.00	10.12	−0.43	9.69	0.00
GG-A	4.23	−0.50	3.73	0.15	3.92	−0.56	3.35	0.21
GG-B	2.61	−0.72	1.90	3.43	2.37	−1.22	1.15	8.61
GG-C	1.53	−0.36	1.17	11.52	1.42	−0.93	0.49	26.46
GG-E	6.96	−1.24	5.71	0.01	6.31	−1.18	5.13	0.01
GG-F	6.89	0.66	7.55	0.00	5.26	0.30	5.56	0.00
GG-M	7.12	−0.67	6.45	0.00	6.89	−1.48	5.40	0.01

[a] $\Delta U_{T=0\,K} = U_{T=0\,K}(\text{conf X}) - U_{T=0\,K}(\text{conf TG-A})$. For conformer TG-A, $U_{T=0\,K} = -1290.721085$ a.u.
[b] $\Delta G_{corr} = G_{corr}(\text{conf X}) - G_{corr}(\text{conf TG-A})$, where $G_{corr} = G^0_{T=298.15\,K} - U_{T=0\,K}$; ΔG_{corr} corresponds to the difference for two conformers of thermal and entropic corrections that convert the internal energy (U) to the Gibbs-free energy (G). For conformer TG-A, $\Delta G_{corr} = 0.351282$ a.u.
[c] $\Delta G^{gas}_{final} = G^0_{T=298.15\,K}$ for conformers in gas-phase, and given by $\Delta U_{T=0\,K} + \Delta G_{corr}$.
[d] $\Delta U_{T=0\,K} = U_{T=0\,K}(\text{conf X}) - U_{T=0\,K}(\text{conf TG-A})$. For conformer TG-A, $U_{T=0\,K} = -1298.0236255$ a.u.
[e] For conformer TG-A, $\Delta G_{corr} = 0.316810$ a.u.

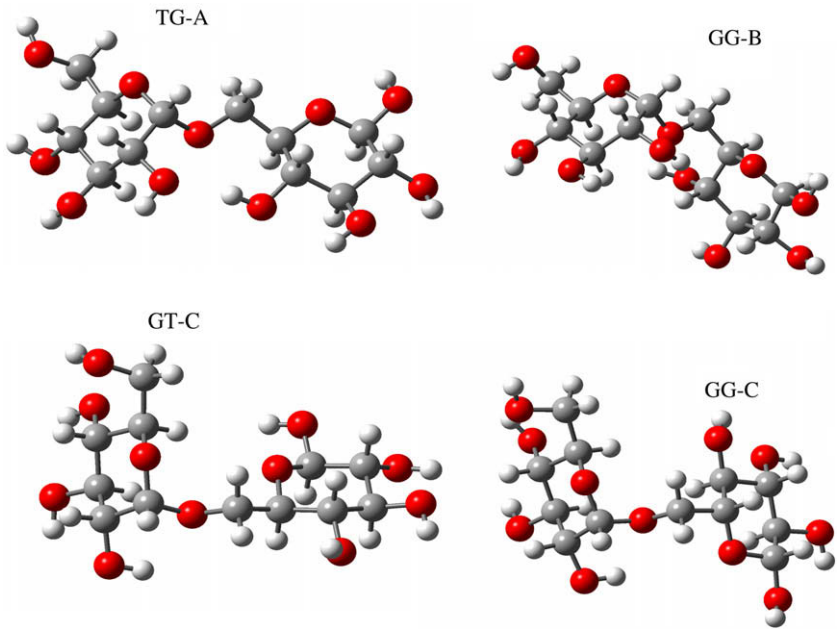

Figure 6. Most stable conformations found for β-isomaltose calculated as isolated molecule at HF/6-31G(d,p). As can be seen, all structures kept a *gg* orientation of the hydroxymethyl groups, despite all geometrical optimizations.

Table 4
Relative abundance of each orientation along the glycosidic bond

Calculation level	TG (A)	GG (B + C)	GT (C)
HF//6-31G(d,p)	84%	15%(3%+12%)	1%
B3LYP/6-311+G(2d,2p)//HF/6-31G(d,p)	54%	38%(14%+24%)	6%
B3LYP//6-31+G(d,p)	61%	35%(9%+26%)	4%
B3LYP/6-311+G(2d,2p)//B3LYP/6-31+G(d,p)	33%	57%(19%+38%)	9%

hydrogen bond between the hydroxyl groups of carbon atoms 4 and 6, generating what the authors call the attractive and repulsive potential energy curves. The authors assumed that as the hydrogen bond formation with the solvent may compete with the intramolecular hydrogen bonds, the repulsive energy curves for the isolated system could describe the removal of the intramolecular hydrogen bond stabilization and, consequently, would be a model

for the influence of solvation (but only to the extent that solvation totally removes intramolecular hydrogen bonds). This assumption is due to the shape of the repulsion potential curve obtained which shows the TG rotamer as a non-abundant structure for methyl α-D-glucopyranoside, in agreement with the experimental study available in aqueous solution.[22]

The extrapolation of these assumptions to glycosidic bonds as suggested by the authors, however, deserves care and attention. From Table 4, it can be seen that even in the absence of solvation, TG conformers are less stable, and this behavior is obtained when electronic correlation effects are properly taken into account. It is not a consequence of intramolecular hydrogen bonds replaced by intermolecular bonds, established in a solute–solvent interaction context. When solvation effects are introduced, we will return to this discussion.

Returning to analyze the behavior of monosaccharides, the authors also call attention to the fact that the quantum mechanical curves obtained exchange the ordering of the relative abundance of GT:GG for methyl α-D-glucopyranoside (62:37) when the same experimental results are considered (38:57).[22] This is different from molecular mechanics results, which agree better with this set of experimental data (40:54). However, it is not possible to forget that other theoretical studies[37,18,17] have found also a similar GT over GG populational prevalence for α-glucose (and also for the β anomer) in aqueous solution, furnishing this set of conformers optical rotation theoretical values and a rate coefficient of mutarotation in very good agreement with experiments.

In order to study the solvent effects on this set of 18 conformers, single point calculations were performed at B3LYP/6-31+G(d,p) using the PCM dielectric continuum approach, on geometries optimized at the same level of theory in the gas-phase. The results are reported in Table 5.

First of all, it is worthwhile to mention that although PCM is basically an electrostatic model the conformers with highest dipole moments are not always the most abundant structures. It means that other effects besides those of pure electrostatic nature are taking place. If the solvation model adopted properly quantitatively computes all of them or not will depend on how good is the agreement with the experiments. But we can verify from these results that PCM model is not insensitive to this.

The minimum energy regions in the gas-phase are the same also in PCM. Solvation, at least to the extent considered here, is not able to overcome intramolecular effects, becoming a non-stable gas-phase conformer, a stable structure in PCM. However, important changes in the energy are observed and the relative abundance of conformers changes very much. The data in Table 5 show that the orientation along the glycosidic linkage (compared at B3LYP/6-31+G(d,p) level) changes the relative TG:GG:GT abundance from 61:35:4 in the gas-phase to 85:9:6 in PCM. Introduction of solvation effects through PCM model, contrary to that proposed by Kirschner and Woods[21] for the hydroxymethyl group, enlarges the TG and GT relative abundance, while diminishing the GG. Such behavior is also in opposition to experimental results, which suggest the 1:70:29 relative abundance for α-isomaltose in D_2O.[38] It is important to keep in mind that these values were obtained from experimental $J_{H5,H6R'}$ and $J_{H5,H6S'}$ for the α-isomaltose, a set of coupling constants much more sensitive to the C1 anomeric conformation, as will be made clear in the next sections. The relative conformational abundance was obtained from homonuclear H5,H6R and H5,H6S spin coupling constants, replaced in the Serianni and coworkers' equation, developed from NMR data of hydroxymethyl orientations in methyl pentofuranosides.[39] Comparing Nishida et al.[22] experimental results for monosaccharides with those of Ohrui et al.[38] for disaccharides, it can be seen that the TG is always an unfavorable orientation (along the glycosidic linkage and to the hydroxymethyl group), while GG seems to prevail over GT.

In order to look for a reduction of the TG conformers abundance, and before going beyond the B3LYP/6-31+(d,p) single point description for the solvent effects, it is time to look at the possible hydroxymethyl orientations, because all conformers we have studied up to now have this group into the *gg* one.

Table 5
Glycosidic angles (in degrees), relative energies (in kcal/mol), Boltzmann population and dipole moment (in debye) for the 18 conformers obtained from conformational maps of Figures 3–5, after B3LYP/6-31+G(d,p) single point calculations in PCM, on geometries optimized in the gas-phase

Region	ϕ	ψ	ΔG_{sol}[a]	ΔG_f^{sol}[b]	p^{sol} (%)	μ^{sol}
TG-A	82	154	0.00	0.00	84.37	8.7
TG-B	93	109	3.70	3.74	0.15	7.7
TG-C	76	244	4.54	3.83	0.13	5.5
TG-E	105	297	5.14	5.57	0.01	4.9
TG-J	146	262	5.49	4.48	0.04	6.8
TG-L	267	185	9.31	8.59	0.00	7.2
GT-B	97	75	2.34	2.43	1.39	4.1
GT-C	67	194	2.82	1.66	5.08	4.9
GT-E	92	295	5.40	4.59	0.04	6.0
GT-I	142	189	6.17	4.30	0.06	4.6
GT-L	107	285	7.21	6.09	0.00	4.4
GT-N	299	220	8.13	7.70	0.00	5.9
GG-A	78	83	5.61	5.05	0.02	9.1
GG-B	77	161	2.78	1.56	6.07	2.5
GG-C	72	178	3.19	2.25	1.87	6.9
GG-E	143	193	6.56	5.38	0.01	4.3
GG-F	94	247	3.23	3.53	0.22	2.0
GG-M	67	89	4.46	2.98	0.55	10.5

[a] $\Delta G_{sol} = G_{sol}(\text{conf X}) - G_{sol}(\text{conf TG-A})$, where G_{sol} is the conformer energy in aqueous solution. For conformer TG-A, $G_{sol} = -1298.051776$ a.u.
[b] $\Delta G^{sol}_{final} = \Delta G^{0}_{T=298.15K}$ in aqueous solution, and given by $\Delta G_{sol} + \Delta G_{corr}$ (in the gas-phase).

3.3. The rotation of the hydroxymethyl groups

In the investigation of the other possible orientations for the hydroxymethyl group, and how they affect the dihedral angles of the glycosidic linkage, eight new additional structures were considered, assuming that the glycosidic angles of structures different from TG-A, GT-C, GG-B, and GG-C are not favored. They were obtained from the four optimized conformers mentioned (the most abundant species found in the gas-phase and aqueous solution), which have all a *gg* orientation (see Fig. 6). By proper rigid rotations, two sets of four new starting structures were created, named TG-A-*tg*, GT-C-*tg*, GG-B-*tg*, and GG-C-*tg*, and TG-A-*gt*, GT-C-*gt*, GG-B-*gt*, and GG-C-*gt*. The geometries of these eight structures were optimized in the gas-phase (B3LYP/6-31+G(d,p)) and the analytical frequencies calculated. Solvation energies were obtained from single point calculations at B3LYP/6-31+G(d,p) and B3LYP/6-311+G(d,p) levels, on geometries optimized in the gas-phase. Additionally, geometry optimizations (B3LYP/6-31+G(d,p)) in PCM were conducted, and single point calculations in PCM at the B3LYP/6-311+G(2d,2p) level on them were also performed. These data, which can be found in the Supplementary data, provided the following discussion, which will be conducted presenting the effects on the geometries separately from those on the energy.

3.3.1. Isolated system x in PCM optimized geometries

Table 6 reports the main geometrical optimized parameters (ϕ, ψ, Ω, and ω) of the structures calculated as isolated system and in PCM.

The ϕ glycosidic angle, defined by the exo-anomeric effect, is kept around 60° for all GG, GT, and TG structures presenting this last glycosidic orientation the largest deviation (the values are

Table 6
Main geometrical parameters (ϕ, ψ, Ω, and ω in degrees) optimized for the conformers calculated in the gas-phase and in PCM at B3LYP/6-31+G(d,p) level

Conformer	Gas-phase				PCM			
	ϕ	ψ	Ω	ω	ϕ	ψ	Ω	ω
TG-A-*gg*	82	154	180	277	80	154	180	291
TG-A-*gt*	80	156	181	75	82	153	179	71
TG-A-*tg*	83	153	179	181	81	153	180	179
GT-C-*gg*	67	194	72	283	72	170	71	295
GT-C-*gt*	66	174	71	59	73	171	71	62
GT-C-*tg*	68	231	79	158	71	231	78	156
GG-B-*gg*	77	161	293	283	75	156	293	295
GG-B-*gt*	76	204	300	61	77	205	299	62
GG-B-*tg*	76	171	295	164	77	160	295	168
GG-C-*gg*	72	178	295	277	72	180	294	292
GG-C-*gt*	71	166	296	73	76	160	295	70
GG-C-*tg*	72	179	295	181	72	178	294	179

around 80°). The ψ angle is the geometrical parameter that presents the largest variation among the set of conformers studied, and in the GT-C and GG-B conformers it is a degree of freedom very sensitive to the hydroxymethyl orientation. The Ω dihedral angle is kept around 180°, 60°, and 300° for TG, GT, and GG glycosidic orientations, as expected, similarly to the *tg*, *gt*, and *gg* hydroxymethyl orientations, when the ω angle assumes the same corresponding values. Solvation effects, however, seem to enlarge the ω values for the *gg* conformers.

In general, the geometry of the conformers is very similar in the gas-phase and in PCM, although an exception is made for the ψ glycosidic angle of the GT-C-*gg* conformer.

3.3.2. Isolated system x in PCM conformational abundance

Table 7 shows the relative abundance, obtained as a Boltzmann distribution of the twelve conformers considered, in different theoretical levels. All energy data needed to obtain the reported values are available in the Supplementary data.

For the isolated system, which takes into account only intramolecular effects, from Table 7 it can be seen that the relative abundance TG:GT:GG is 40:13:46 for the orientation along the glycosidic bond, an improvement of the distribution presented in Table 4 (61:4:35) if the experimental result[38] is assumed as the benchmark (1:29:70). It means that other orientations besides *gg* must be considered, a confirmation that the hydroxymethyl rotation is a very important degree of freedom for β-isomaltose that cannot be neglected in conformational studies. However, the population found for the hydroxymethyl moiety when only intramolecular effects are considered is 68:26:5 (*tg*:*gt*:*gg*), and we can clearly see that it is a distinct distribution from that obtained for the glycosidic orientation, presenting the former a *tg* > *gt* > *gg* prevalence, while the latter is GG > TG > GT. These results suggest that when only intramolecular effects are taken into account, the dominating effects that stabilize the hydroxymethyl orientations are different from those that make the glycosidic α-(1,6) linkage, and extrapolations from hydroxymethyl behavior to 1,6 glycosidic bond in carbohydrates must be avoided.

In order to compare the results obtained with experimental data, solvation must be included. In doing this, the orientation along the glycosidic bond shifts to 79:13:8 (TG:GT:GG) if single point calculations are performed at the same level on the gas-phase optimized geometries. If optimization in PCM is performed at the same level, instead, the numbers are 65:27:8. Still taking the isolated system geometry as reference, electronic correlation effects in single point PCM calculations change such relative abundance from 40:13:46 to 79:13:8 or even to 76:15:9, depending of the basis set size. Finally, if a large basis set is used on geometries optimized in PCM, the final population is 39:49:12. Such data show that while solvation effects stabilize TG, electronic correlation inclusion destabilizes such glycosidic orientation. Concomitantly, solvation effects disfavor GG orientation, while electronic correlation favors it slightly. Finally, GT glycosidic orientation seems to be the most favored, being stabilized not only in energy but also by the geometrical changes induced by the solute–solvent interactions (see Table 6), in addition to the stabilization that comes from the recovery of the electronic correlation effects. The final effect is that GT-C-*gg* conformer becomes the global minimum or the most abundant conformation in aqueous solution, at least at the highest level of description adopted here.

With respect to this degree of freedom, Pérez and co-workers[5] found through a semi-empirical method a relative abundance of 18:30:52 (TG:GT:GG), very different from ours. Considering the study performed by French and co-workers,[3] if we assume a

Table 7
Boltzmann population (%) for the 12 conformers optimized at B3LYP//6-31+G(d,p) level, in the gas-phase and in PCM

	Gas-phase	PCM			
	B3LYP//6-31+G(d,p)	B3LYP/6-31+G(d,p)[a]	B3LYP/6-311+G(d,p)[a]	B3LYP//6-31+G(d,p)	B3LYP/6-311+G(2d,2p)[b]
TG-A-*gg*	3.22	7.56	8.19	12.73	10.09
TG-A-*gt*	0.27	13.31	14.26	12.58	11.50
TG-A-*tg*	37.01	57.99	54.06	39.91	17.74
GT-C-*gg*	0.20	0.45	0.58	10.56	26.10
GT-C-*gt*	1.90	11.30	12.38	8.95	18.72
GT-C-*tg*	11.06	1.63	1.62	7.28	4.37
GG-B-*gg*	0.46	0.54	0.76	0.28	0.66
GG-B-*gt*	24.09	2.58	2.65	4.79	6.48
GG-B-*tg*	7.74	1.24	1.52	2.48	3.69
GG-C-*gg*	1.42	0.17	0.21	0.07	0.14
GG-C-*gt*	0.12	0.92	1.15	0.09	0.20
GG-C-*tg*	12.52	2.29	2.63	0.28	0.30
TG	40	79	76	65	39
GT	13	13	15	27	49
GG	46	8	9	8	12
tg	68	63	60	50	26
gt	26	28	30	26	37
gg	5	9	10	24	37

[a] Single point calculations in PCM, on the geometry optimized in the gas-phase.
[b] Single point calculations in PCM, on the geometry optimized in PCM.

Boltzmann distribution for the relative energy values presented in Table 1, a 5:53:41 relative population is obtained. Naidoo and co-workers[2] (also assuming a Boltzmann distribution for the relative energy values exhibited in their Table 3) reported a 0:66:34 abundance, obtained from molecular dynamics simulations with Palma et al. force field.[40] Hünenberger and co-workers[4] reported a 0:56:44 relative abundance, for a molecular mechanics study using GROMOS 45A4 force field,[41] recently developed for carbohydrates.

Looking to the other important molecular movement related to the hydroxymethyl group rotation, some considerations can be drawn from Table 7, regarding the relative abundance of the conformers studied. Again assuming the isolated system as the reference because only intramolecular effects are present in the molecule stabilization, we can see that the *tg:gt:gg* conformational abundance is of 68:26:5. These populations are shifted to 63:28:9 and 50:26:24 if solvation effects are taken into account in single point calculations on the gas-phase optimized geometries, and in geometry optimization calculations performed in PCM, respectively. If electronic correlation is introduced with larger basis sets on both descriptions, the numbers change to 60:30:10 and 26:37:37, respectively. Here, the *tg* population is reduced by solvation and consideration of electronic correlation, while the *gg* hydroxymethyl orientation is proportionally enlarged. The *gt* orientation is much less sensitive to such effects. The final distribution we have found is that in aqueous solution the *gt* and *gg* are equally abundant, and that although the *tg* orientation is disfavored by solvation and electronic correlation effects, in agreement with Kirschner and Woods,[21] it never becomes a negligible conformation as proposed by those authors and also by experiments.[22] It is important to recall, however, that the two later mentioned studies were performed for monosaccharides.

The conformational sampling protocol adopted here, tacitly assumes that the rotation of the glycosidic bond changes the energy of the system more drastically than the rotation of the hydroxymethyl groups, being a degree of freedom more important than the latter. To confirm this assumption, the mean value of the energy differences among the 18 conformers shown in Tables 3–5 are, respectively, 5.33, 4.27, and 4.09 kcal/mol, for HF//6-31G(d,p), B3LYP//6-31+G(d,p) in the gas-phase and B3LYP/6-31+G(d,p) in the continuum (in single-point calculations of the geometries optimized at the same level in the gas-phase). The corresponding values for the 12 conformers are 2.88, 1.63, and 1.89 kcal/mol (see Tables in the Supplementary data). It means that the hydroxymethyl rotation changes the energy of the β-isomaltose less than a similar movement in the glycosidic linkage, and can therefore be considered 'subminima' inside the regions of the minimum energy of the corresponding conformational maps.

The conformers that in Table 7 have a relative abundance in PCM at B3LYP/6-311+G(2d,2p)//B3LYP/6-31+G(d,p) level higher than 1% are shown in Figure 7.

It must be mentioned that an anticlock orientation of all hydroxyl groups was investigated, in order to consider the cooperativity effect, as proposed by Klein[42] for monosaccharides. However, for β-isomaltose, this procedure furnished a set of conformers with higher energy values than those considered in the previous discussion.

In a 1,6 glycosidic bond, the monosaccharidic rings can stay more distant from each other than in other glycosidic bonds, exploiting a larger number of conformations stabilized by inter residue hydrogen bonds, due to several geometrical arrangements accessible to a 1→6 bond but impossible for other bonds. Such interactions are well represented by the influence of the hydroxymethyl orientation on the glycosidic angles, well represented in GT-C-*tg* and GG-B-*gt* conformations shown in Figure 7.

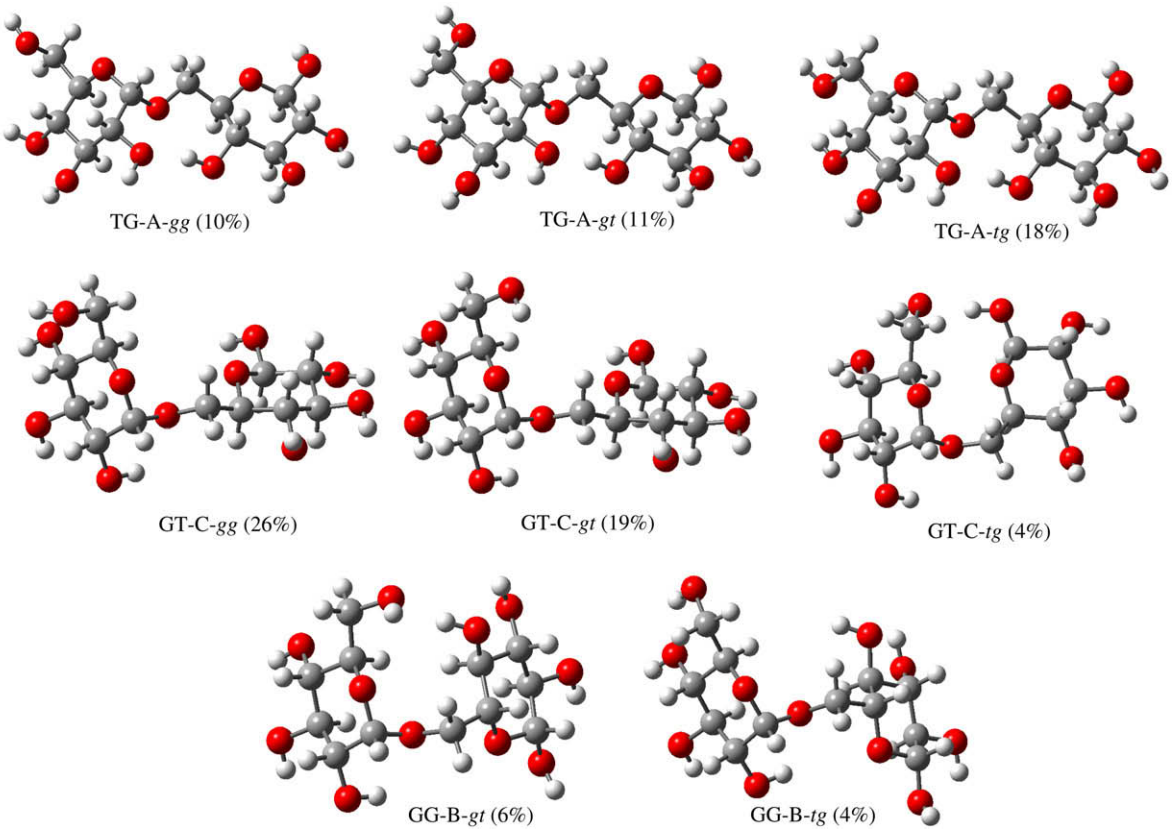

Figure 7. Most stable conformations found for β-isomaltose in PCM at B3LYP/6-311+G(2d,2p)//B3LYP/6-31+G(d,p) level of calculation. Relative abundance is reported between parentheses.

Here we would rather not explicitly identify hydrogen bonds between the atoms and attribute stabilization exclusively to them because almost all conformers can present such an inter residue interaction, making it difficult to present a quantitative argument. Instead of this, we have preferred to look at the geometries of the conformers *after* the energy results are analyzed.

3.4. Calculation of the heteronuclear spin coupling constants ($^3J_{C,H}$)

To validate the conformational sampling performed in this study, $^3J_{C,H}$ were calculated for the atoms along the glycosidic bond for each individual conformer, as explained in previous sections. The Boltzmann population obtained in PCM was used in a weighted average to furnish the theoretical heteronuclear spin coupling constants ($^3J_{C,H}$) final value. The results are shown in Tables 8 (validation of the ψ angle) and 9 (validation of the Ω angle). The atomic labels follow the indications of Figure 1.

From Tables 8 and 9, it can be seen that the agreement between quantum mechanical values of $^3J_{C,H}$ and those obtained from a Karplus-type equation is much better for the atoms of the C1–O1–C6′–C5′ sequence (Table 8), than for those of the C4′–C5′–C6′–H6′ (R or S) sequence. As the extension of the basis set (here limited by system dimension) it is important to assure reliable values of *J*, in the latter we will use only the Karplus-type values to perform comparisons with experimental values.

This kind of coupling constant does not have a very high value and the differences found in Table 8 are acceptable. In fact, it is proposed in the literature[43] that a better choice would be to use $^3J_{H5,H6R}$ and $^3J_{H5,H6S}$ values. For *tg* and *gt* orientations, they have a very high value at least for one of such properties (approximately 10 Hz). However, these values are not available in the literature for the β-isomaltose anomer, to the best of our knowledge.

Therefore, a better comparison between the theoretical value for $^3J_{C,H}$ coupling constants found in this study with those also found in other theoretical studies as well as with the experimental benchmark is made in Table 10.

As can be seen from the previous table, the agreement with experimental results is achieved for two values of $^3J_{C,H}$ ($^3J_{C'6,H1}$ and $^3J_{C1,H6S'}$) that refer to ψ angle, but not for $^3J_{C1,H6R'}$. Also in regard to the Ω angle, only one value ($^3J_{C4',H6S'}$) provides a reasonable agreement. Here some considerations can take place because a similar behavior is observed from Pérez and co-workers' study.[5] It seems that only one of the two experimental $^3J_{C,H6'}$ values can be reproduced, and the difficulty in the experimental determination of both values cannot be forgotten.[43] Because both protons are bonded to the same carbon atom, it would be very hard to theoretically find a set of conformers able to reproduce only one of them (even through an average value). Due to such findings and taking into account that there is only one set of experimental data available, we may consider the agreement acceptable and, therefore, that the set of conformers cannot be said to be non-representative for the β-isomaltose compound in an aqueous solution. We may also take this opportunity to call attention to the scarce source of $^3J_{C,H}$ and principally $^3J_{H,H}$ data for the α-1,6 glycosidic bond.

Table 8
Boltzmann populations in solution, ϕ dihedral angles (in degrees) and individual heteronuclear spin coupling constants ($^3J_{C,H}$ in Hz) for each conformer in Table 6, obtained from a Karplus-type equation (KE), and from quantum mechanical (QM) calculations at B3LYP//6-31+G(d,p) level in PCM

Conformer	p_i^{sol} (%)	ϕ_{H1}	$\phi_{H6S'}$	$\phi_{H6R'}$	KE			QM		
					$^3J_{C'6,H1}$	$^3J_{C1,H6S'}$	$^3J_{C1,H6R'}$	$^3J_{C'6,H1}$	$^3J_{C1,H6S'}$	$^3J_{C1,H6R'}$
TG-A-*gg*	10.09	322	35	274	3.57	3.83	0.49	3.98	3.88	−0.26
TG-A-*gt*	11.50	324	34	273	3.75	3.92	0.48	4.14	3.92	−0.27
TG-A-*tg*	17.74	324	34	274	3.75	3.92	0.49	4.13	3.91	−0.27
GT-C-*gg*	26.10	315	50	291	2.93	2.47	1.02	3.33	2.38	0.19
GT-C-*gt*	18.72	316	51	291	3.02	2.38	1.02	3.39	2.25	0.27
GT-C-*tg*	4.37	314	112	352	2.83	1.52	5.50	3.21	1.77	5.76
GG-B-*gg*	0.66	318	36	277	3.20	3.75	0.51	3.71	3.44	−0.22
GG-B-*gt*	6.48	320	85	325	3.39	0.49	3.83	4.12	0.01	4.90
GG-B-*tg*	3.69	320	40	280	3.39	3.39	0.57	3.88	3.02	−0.12
GG-C-*gg*	0.14	315	60	300	2.93	1.62	1.63	3.33	1.13	1.29
GG-C-*gt*	0.20	319	40	280	3.29	3.39	0.57	3.67	3.03	−0.13
GG-C-*tg*	0.30	315	58	298	2.93	1.78	1.47	3.41	1.30	1.11
Weighted average					3.29	2.89	1.17	3.71	2.80	0.56

Table 9
Boltzmann populations in solution, ϕ dihedral angles (in degrees) and individual heteronuclear spin coupling constants ($^3J_{C,H}$ in Hz) for each conformer in Table 6, obtained from a Karplus-type equation (KE), and from quantum mechanical (QM) calculations at B3LYP//6-31+G(d,p) level in PCM

Conformer	p_i^{sol} (%)	$\phi_{H6S'}$	$\phi_{H6R'}$	KE		QM	
				$^3J_{C4',H6S'}$	$^3J_{C4',H6R'}$	$^3J_{C4',H6S'}$	$^3J_{C4',H6R'}$
TG-A-*gg*	10.09	59	179	1.46	7.91	2.56	5.73
TG-A-*gt*	11.50	58	178	1.54	7.89	2.65	5.76
TG-A-*tg*	17.74	59	178	1.46	7.89	2.62	5.73
GT-C-*gg*	26.10	310	70	1.63	0.81	0.64	0.78
GT-C-*gt*	18.72	310	70	1.63	0.81	0.64	0.75
GT-C-*tg*	4.37	318	76	2.27	0.58	0.52	0.44
GG-B-*gg*	0.66	174	293	7.79	0.60	4.10	0.32
GG-B-*gt*	6.48	181	300	7.93	0.94	4.45	0.53
GG-B-*tg*	3.69	176	295	7.85	0.68	4.17	0.38
GG-C-*gg*	0.14	176	295	7.85	0.68	3.96	0.30
GG-C-*gt*	0.20	177	296	7.87	0.73	4.05	0.36
GG-C-*tg*	0.30	177	296	7.87	0.73	3.99	0.32
Weighted average				2.32	3.59	1.83	2.67

Table 10
Experimental and theoretical $^3J_{C,H}$ values (in Hz), obtained from a Karplus-type equation (a) or ab initio calculations (b)

Parameter	This work	MM3[3]	Semi-empirical[5]	Exp.[44]
$^3J_{C'6,H1}$	3.29[a]; 3.71[b]	3.1	3.2	3.6
$^3J_{C1,H6S'}$	2.89[a]; 2.80[b]	1.4	1.6	2.4
$^3J_{C1,H6R'}$	1.17[a]; 0.56[b]	2.3	3.1	2.9
$^3J_{C4',H6S'}$	2.32[a]	—	—	2.45[c]
$^3J_{C4',H6R'}$	3.59[a]	—	4.68	1.0[c]

[c] Experimental values for methyl 6-*O*-methyl-β-D-glucopyranoside.[32]

4. Conclusions and perspectives

In this study we have considered the most stable conformations of β-isomaltose molecule using ab initio and density functional calculations. Three conformational maps regarding TG, GT, and GG glycosidic orientations were obtained at the HF/6-31G(d,p) level. From the sampling of these potential energy surfaces, 18 stable structures were obtained at the end of the procedure. Hydroxymethyl group orientation was investigated at the B3LYP level with different basis sets, sampling the most stable regions at 298 K found in the previous step.

For all the stable conformations obtained, the variation of the ϕ angle is smaller than the variation of the ψ angle, proving the influence of the exo-anomeric effect in the restriction of the rotation of the ϕ angle. Compared to other glycosidic linkages, it can be said that a (1→6) bond is much more conformationally versatile, existing in many possible stable conformations. The consideration of electronic correlation effects favors the GG glycosidic orientation and not the TG. Solvation has an opposite influence. The GT orientation is not very affected by electronic correlation recovering but is very stabilized by solvation effects not only in geometry but also in energy.

Solvation effects do not give rise to new regions of stability. However, there is a variation in the relative abundance of conformers from the gas-phase to aqueous solution. Thus, it can be said that the intramolecular effects determine conformation, while the intermolecular effects (solvation) determine relative abundance. Any analysis of them should be conducted separately or learning about the system behavior could be misunderstood.

The hydroxymethyl group rotations (∼C–C∼ bond) react differently to the glycosidic linkage rotations (∼C–C∼ bond) with respect to the electronic correlation recovering and solvation effects introduction, precluding any extrapolation from monosaccharide conformational studies to disaccharides. Solvation stabilizes the *gg* conformers very much, while the *tg* conformers are largely disfavored by both effects.

To assure that the presented conformers are the most stable for β-isomaltose would be premature without a more detailed investigation on the hydroxyl groups orientations. However, we believe that the selected set is representative concerning the glycosidic orientation.

The energetic differences between rotations of the glycosidic bond and hydroxymethyl groups suggest that a hierarchy can exist between such molecular degrees of freedom, this achievement also being observed in previous conformational studies performed for trehalose[16] and β-lactose.[15] This fact can allow a decoupling of movement, used as a search criteria in conformational sampling on potential energy surfaces. As solvation reduces the energy barriers it would be interesting to obtain quantum mechanical conformational maps considering solvation effects (work in progress).

Considering the conformational maps obtained, as well as others already published,[44] it is time to state that as the type of glycosidic linkage defines the disaccharide conformation, therefore, only force fields parameterized by types of glycosidic bond will be able to describe oligo and polysaccharides properly. The robustness of such parameterization will be dictated by the quality of the conformational maps used to perform it and ab initio conformational maps would be an unbiased choice.

Experimental values for disaccharides in solution are able to furnish ONLY average conformational information, therefore any force field parameterization that uses them may provide non-reliable results, because it will be based on conformations of non-physical occurrence. If the Boltzmann distribution is unknown, it is not possible to access individual conformations from experimental data. Therefore, theoretical studies on carbohydrates can have a particular role in answering such questions.

Acknowledgments

The authors would like to thank FAPERJ, CAPES and CNPq for their financial support given to this study.

Supplementary data

Supplementary data (complete geometrical coordinates and electronic energies for the conformers) associated with this article can be found, in the online version, at doi:10.1016/j.carres.2009.04.022.

References

1. Rao, V. S. R.; Qasba, P. K.; Balaji, P. V.; Chandrasekaran, R. *Conformation of Carbohydrates*; Harwood Academic: Amsterdam, 1998.
2. Best, R. B.; Jackson, G. E.; Naidoo, K. J. *J. Phys. Chem. B* **2001**, *105*, 4742–4751.
3. Dowd, M. K.; Reilly, P. J.; French, A. D. *Biopolymers* **1994**, *34*, 625–638.
4. Pereira, C. S.; Kony, D.; Baron, R.; Müller, M.; van Gunsteren, W. F.; Hünenberger, P. H. *Biophys. J.* **2006**, *90*, 4337–4344.
5. Tvaroska, I.; Imberty, A.; Pérez, S. *Biopolymers* **1990**, *30*, 369–379.
6. Bitzer, R. S.; Barbosa, A. G. H.; Silva, C. O.; Nascimento, M. A. C. *Carbohydr. Res.* **2005**, *340*, 2171–2184.
7. Woods, R. J.. In *Reviews in Computational Chemistry*; Lipkowitz, K. B., Boyd, D. B., Eds.; VCH: New York, 1996; Vol. 9, pp 129–165.
8. Hemmingsen, L.; Madsen, D. E.; Esbensen, A. L.; Olsen, L.; Engelsen, S. B. *Carbohydr. Res.* **2004**, *339*, 937–948.
9. Pérez, S.; Imberty, A.; Engelsen, S. B.; Gruza, J.; Mazeau, K.; Jiménez-Barbero, J.; Poveda, A.; Espinosa, J.-F.; van Eyck, B. P.; Johnson, G.; French, A. D.; Kouwijzer, M. L. C. E.; Grootenius, P. D. J.; Bernardi, A.; Raimondi, L.; Senderowitz, H.; Durier, V.; Vergoten, G.; Rasmussen, K. *Carbohydr. Res.* **1998**, *314*, 141–155.
10. Bosma, W. B.; Appell, M.; Willet, J. L.; Momany, F. A. *J. Mol. Struct. (THEOCHEM)* **2006**, *776*, 1–19.
11. Bosma, W. B.; Appell, M.; Willet, J. L.; Momany, F. A. *J. Mol. Struct. (THEOCHEM)* **2006**, *776*, 21–31.
12. Lemieux, R. U.; Koto, S. *Tetrahedron* **1974**, *30*, 1933–1944.
13. French, A. D.; Kelterer, A.-M.; Johnson, G.; Dowd, M. K.; Cramer, C. J. *J. Comput. Chem.* **2001**, *22*, 65–78.
14. French, A. D.; Kelterer, A.-M.; Johnson, G. P.; Dowd, M. K.; Cramer, C. J. *J. Mol. Graphics Modell.* **2000**, *18*, 95–107.
15. Silva, C. O.; Nascimento, M. A. C. *Carbohyd. Res.* **2004**, *339*, 113–122.
16. Soares, C. S.; Silva, C. O. *Quim. Nova* **2008**, *31*, 280–284.
17. Silva, A. M.; Silva, E. C.; Silva, C. O. *Carbohydr. Res.* **2006**, *341*, 1029–1040.
18. Silva, C. O.; Vreven, T.; Mennucci, B. *J. Org. Chem.* **2004**, *69*, 8161–8164.
19. *Continuum Solvation Models in Chemical Physics: From Theory to Applications*; Mennucci, B., Cammi, R., Eds.; Wiley & Sons, 2007.
20. Umeyama, H.; Morokuma, K. *J. Am. Chem. Soc.* **1977**, *99*, 1316–1332.
21. Kirschner, K. N.; Woods, R. J. *PNAS* **2001**, *98*, 10541–10545.
22. Nishida, Y.; Ohrui, H.; Meguro, H. *Tetrahedron Lett.* **1984**, *25*, 1575–1578.
23. Woods, R. J.; Dwek, R. A.; Edge, C. J.; Fraser-Reid, B. *J. Phys. Chem.* **1995**, *99*, 3832–3846.
24. Csonka, G. I. J. *Mol. Struct. (THEOCHEM)* **2002**, *584*, 1–4.
25. Lii, J.-H.; Ma, B.; Allinger, N. L. *J. Comput. Chem.* **1999**, *15*, 1593–1608.
26. Cammi, R.; Tomasi, J. *J. Comput. Chem.* **1995**, *16*, 1449–1458.
27. Mennucci, B.; Cancès, E.; Tomasi, J. *J. Chem. Phys.* **1997**, *107*, 3032–3041.
28. Bondi, A. *J. Phys. Chem.* **1964**, *68*, 441–451.
29. JAGUAR *6.0*; Schrödinger: Portland, OR, USA, 2006.
30. Frisch, M. J. et al GAUSSIAN *03 (Revision C.01)*; Gaussian: Pittsburg, PA, 2003.
31. Tvaroska, I.; Hricovini, M.; Petrakova, E. *Carbohydr. Res.* **1989**, *189*, 359–362.
32. Tvaroška, I.; Taravel, F. R.; Utille, J. P.; Carver, J. P. *Carbohydr. Res.* **2002**, *337*, 353–367.
33. Helgaker, T.; Watson, M.; Handy, N. C. *J. Chem. Phys.* **2000**, *113*, 9402–9409.
34. Sychrovsky, V.; Grafenstein, J.; Cremer, D. *J. Chem. Phys.* **2000**, *113*, 3530–3547.

35. Barone, V.; Peralta, J. E.; Contreras, R. H.; Snyder, J. P. *J. Phys. Chem. A* **2002**, *106*, 5607–5612.
36. POLYGRAF *v3.2.1*; Molecular Simulation, 1992.
37. Barrows, S. E.; Storer, J. W.; Cramer, C. J.; French, A. F.; Truhlar, D. G. *J. Comput. Chem.* **1998**, *19*, 1111–1129.
38. Ohrui, H.; Nishida, Y.; Watanabe, M.; Hori, H.; Meguro, H. *Tetrahedron Lett.* **1985**, *26*, 3251–3254.
39. Wu, G. D.; Serianni, A. .; Barker, R. *J. Org. Chem.* **1983**, *48*, 1750–1757.
40. Palma, R.; Himmel, M. E.; Liang, G.; Brady, J. W. Molecular Mechanics in Cellulases. In *ACS Symposium Series: Glycosyl Hydrolases in Biomass Conversion*; Himmel, M. E., Ed.; ACS: Washington, DC, 2001; Vol. 769,. Chapter 7, pp 112–130.
41. Lins, R. D.; Hünenberger, P. H. *J. Comput. Chem.* **2005**, *26*, 1400–1412.
42. Klein, R. A. *J. Am. Chem. Soc.* **2002**, *124*, 13931–13937.
43. Bock, K.; Duus, J. Ø. *J. Carbohydr. Chem.* **1994**, *13*, 513–543.
44. French, A. D.; Kelterer, A.-M.; Johnson, G. P.; Dowd, M. K.; Cramer, C. J. *J. Comput. Chem.* **2001**, *22*, 65–78.